Proceedings of the 2017 IEEE
International Conference on Robotics and Biomimetics
December 5-8, 2017, Macau SAR, China

Design of a Haptic Master Device for Teleoperation Applications

Kai Xu*, *Member, IEEE*, Bin Zhao, *Student Member, IEEE*,
Shu'an Zhang, Zhaoyu Zhang and Nianzeng Xing

***Abstract*—A haptic device with both force and torque outputs is essential in teleoperation applications. However, researchers do not have sufficient access to such a haptic device due to the facts that the commercially available ones are usually expensive and the state-of-the-art research prototypes are not readily reproducible outside the original laboratories. This paper presents the design and preliminary experimentation of the CombOmni, a haptic device with both force and torque outputs. The CombOmni is constructed from two Sensible Omni haptic devices for teleoperation tasks. The Omni device only provides force outputs and its original structure doesn't allow effective connection between two such units. With minimal modifications and a carefully designed stylus, the CombOmni could be easily built. Kinematics-based design optimizations and the system construction are presented. With the effectiveness of the proposed idea demonstrated via calibration and experimental characterizations in the near future, the CombOmni could become a viable option for a haptic device with both force and torque outputs in a cost-effective way.**

I. Introduction

HAPTIC devices reproduce kinesthetic and tactile sensation between an operator and real/simulated environments. Their forms and theoretical foundations could be very different depending on their specific uses [1]. In teleoperation applications (e.g., robotic surgery), a haptic device on the master side realizes kinesthetic interactions, sensing the kinematic status of its end effector (e.g., a hand-held stylus), while generating programmable and agile wrench outputs (preferably including both force and torque components).

Examining the existing haptic (kinesthetic) devices that can be used for teleoperation, categorization regarding the core function is proposed as follows. It should be noted that an additional end effector (e.g., a gripper) could always be incorporated, resulting in increased number of the device's DoFs (Degrees of Freedom). But the additional DoF is not taken into consideration in the presented categorization. Alternative categorization concerning the control method can be found in [2].

- 3-in-3-out devices sense 3-DoF inputs (usually positions) and generate 3-DoF outputs (usually forces). Commercial examples include the Novint Falcon (Novint Technologies), the delta.3 and the omega.3 (Force Dimension). Examples from academia include the joystick mechanism [3], the DELTA-R device [2], the SHaDe device [4], etc. The SHaDe device only has rotational DoFs and deals with orientation inputs and torque outputs.
- 6-in-3-out devices sense 6-DoF inputs (positions and orientations) and generate 3-DoF outputs (usually forces). Commercial examples mainly include the Omni device (now GeoMagic Touch) and the omega.6 device (Force Dimension). A representative research prototype is the laparoscopic interface [5].
- 6-in-n-out devices sense 6-DoF inputs (positions and orientations) and generate multi-DoF outputs (usually forces and torques components). Early examples include the designs using hybrid serial-parallel structures [6, 7]. Then the delta.6, delta.7 and sigma.7 devices (Force Dimension), as well as the Phantom Premium (GeoMagic) have emerged as commercial products. But they are substantially more expensive than the 6-in-3-out products. Recent research prototypes include the haptic pen [8], the VISHARD6 [9], the PATHOS-II [10], the haptic cobot [11], the modified DELTA-R device (equipped with a 3-DoF rotation mechanism) [2], the CU haptic interface [12], the pinch–grasp haptic interface [13], and the VirtuaPower [14].

Among the existing haptic devices, serial structures are used usually for enlarged workspace, while parallel structures are used for increased stiffness and force output capability. Serial-parallel hybrid structures were also utilized to achieve a balance between proper workspace and adequate stiffness.

6-in-n-out devices are preferred in teleoperation tasks since they generate both force and torque outputs, possibly leading to more faithful interaction between the operator and the haptic device. However, researchers do not have sufficient access to them due to the following reasons. The 6-in-n-out products (usually above USD $50,000 per unit) are substantially more expensive than the 6-in-3-out ones (around USD $ 3,000 per unit), while the state-of-the-art research prototypes are not readily reproducible outside the original laboratories.

This paper hence proposes a convenient solution for the construction of a 6-in-5-out haptic master device, the

Manuscript received July 29, 2017. This work was supported in part by the National Natural Science Foundation of China (Grant No. 51435010, Grant No. 51375295 and Grant No. 91648103), and in part by National Key R&D Program of China (Grant No. SQ2017ZY040208).

Kai Xu is with School of Mechanical Engineering, Shanghai Jiao Tong University, Shanghai, China (asterisk indicates the corresponding author, phone: 86-21-34206547; email: k.xu@sjtu.edu.cn).

Bin Zhao, Shu'an Zhang and Zhaoyu Zhang are with the RII Lab (Lab of Robotics Innovation and Intervention), UM-SJTU Joint Institute, Shanghai Jiao Tong University, Shanghai, China (emails: zhaobin2014@sjtu.edu.cn, jimmyonthego@sjtu.edu.cn and zhangzhaoyu@sjtu.edu.cn).

Nianzeng Xing is with the Department of Urology, Beijing Chaoyang Hospital, Capital Medical University, Beijing, China (email: nianzeng2006@vip.sina.com).

978-1-5386-3742-5/17/$31.00 © 2017 IEEE

CombOmni, for teleoperation tasks, combining two Sensible Omni devices (now called GeoMagic Touch), as shown in Fig. 1. The core motivation is to provide a cost-effective option that is still relatively simple to achieve for researchers who prefer 6-in-n-out haptic devices. The CombOmni is developed with in mind its application in robot-assisted surgeries. It could certainly find applications in other teleoperation tasks.

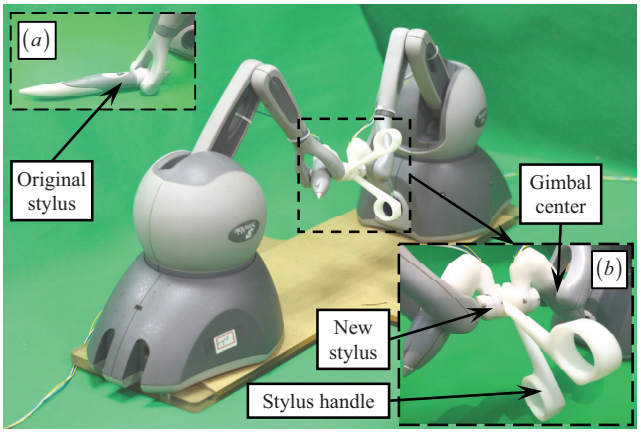

Fig. 1. The constructed CombOmni device: (a) the original stylus, and (b) the new stylus

The CombOmni uses two Omni devices that only provide force outputs. And the original structure of the Omni device doesn't allow effective connection between two such units. Hence the core contributions of this paper lie on the design and kinematics-based optimization of the new stylus that enable effective connection between two Omni devices. The new stylus can be easily printed and installed with minimal modifications to the Omni devices. A similar idea was proposed to use two Novint Falcon devices to provide 5-dimensional force output [15]. Another similar setup using two Omni devices for a master device is in [16]. The CombOmni used an extensively optimized connection to substantially improve its workspace.

This paper is organized as follows. Section II presents the design overview and the kinematics-based optimization of the CombOmni device. The construction of the stylus and the system infrastructure is described in Section III. Preliminary experiments are reported in Section IV, with conclusions and future work summarized in Section V.

II. Design and Optimization of the CombOmni

Since the CombOmni consists of two Omni devices, primary attention was directed to the connection between the two units, in order to effectively utilize the given workspace of one Omni device. Other specifications of the CombOmni, such as resolutions, sampling time, stiffness, force output ranges, etc., would primarily depend on the original specifications of the Omni device.

As explained in the kinematics sections, the Omni device consists of six revolute joints. The proximal three joints (θ_{i1}, θ_{i2} and θ_{i3}) position the gimbal center, while the distal three joints (θ_{i4}, θ_{i5} and θ_{i6}) orient the stylus, as shown in Figs. 1 and 2. If the original styluses of the two Omni devices are directly connected, the CombOmni would have very limited workspace due to the limited motion ranges of the two distal joints (θ_{i4} and θ_{i5}) of the Omni device. A kinematics-based optimization is hence presented in Section II.C for the design of a stylus elbow that better utilizes the joint ranges of the Omni device.

With the stylus elbow designed, the two Omni devices could be connected more effectively. Then another optimization is presented in Section II.D for determining the relative positioning of the two Omni devices to form the CombOmni.

A. Nomenclatures and Coordinates

As shown in Fig. 2, the following coordinates are defined to describe the kinematics of the CombOmni.

- *World Coordinate* $\{W\} \equiv \{\hat{\mathbf{x}}_W, \hat{\mathbf{y}}_W, \hat{\mathbf{z}}_W\}$ is located at the base of the CombOmni, between the two Omni devices.
- *Omni Device Coordinates* $\{Dij\} \equiv \{\hat{\mathbf{x}}_{Dij}, \hat{\mathbf{y}}_{Dij}, \hat{\mathbf{z}}_{Dij}\}$ ($i = 1, 2; j = 0, 1, 2, \cdots, 6$) are assigned to base and the j^{th} link of the i^{th} Omni device according to the Denavit-Hartenberg rules.
- *Stylus Elbow Coordinates* $\{Sik\} \equiv \{\hat{\mathbf{x}}_{Sik}, \hat{\mathbf{y}}_{Sik}, \hat{\mathbf{z}}_{Sik}\}$ ($i = 1, 2; k = 1, 2$) are assigned to the stylus elbow that is installed on the i^{th} Omni device.
- *Handle Coordinates* $\{Hi\} \equiv \{\hat{\mathbf{x}}_{Hi}, \hat{\mathbf{y}}_{Hi}, \hat{\mathbf{z}}_{Hi}\}$ ($i = 1, 2$) are assigned to the CombOmni's stylus handles that are rotatable on the i^{th} Omni device, respectively.

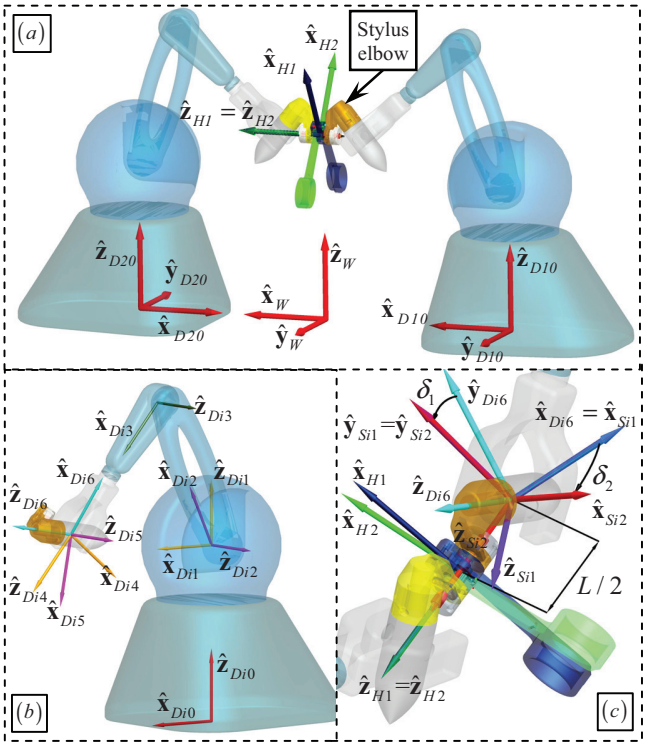

Fig. 2. Coordinates assignment: (a) coordinates of the CombOmni, (b) coordinates of one Omni device, (c) coordinates of the stylus elbow and the stylus handle

B. Kinematics of the Omni Device

As shown in Fig. 2(b), the kinematics of one Omni device can be easily described by assigning seven coordinates referring to the Denavit-Hartenberg rules. For clarity in the visualization of the coordinates in Fig. 2(b), the Y axes are hidden. The homogeneous transformation matrix that relates the adjacent Omni Device Coordinates is as follows.

$$ {}^{Di(j-1)}\mathbf{T}_{Dij} = \begin{bmatrix} {}^{Di(j-1)}\mathbf{R}_{Dij} & {}^{Di(j-1)}\mathbf{p} \\ \mathbf{0}_{1\times3} & 1 \end{bmatrix}, i = 1, 2, j = 1, 2, \cdots, 6 \quad (1) $$

Where $ {}^{Di(j-1)}\mathbf{R}_{Dij} = \begin{bmatrix} \cos\theta_{ij} & -\sin\theta_{ij} & 0 \\ \sin\theta_{ij}\cos\alpha_{j-1} & \cos\theta_{ij}\cos\alpha_{j-1} & -\sin\alpha_{j-1} \\ \sin\theta_{ij}\sin\alpha_{j-1} & \cos\theta_{ij}\sin\alpha_{j-1} & \cos\alpha_{j-1} \end{bmatrix} $

and $ {}^{Di(j-1)}\mathbf{p} = \begin{bmatrix} a_{j-1} & -d_j\sin\alpha_{j-1} & d_j\cos\alpha_{j-1} \end{bmatrix}^T $.

The homogeneous transformation matrix from $\{Di6\}$ to $\{Di0\}$ is obtained as in Eq. (2).

$$ {}^{Di0}\mathbf{T}_{Di6} = \prod_{j=1}^{6} {}^{Di(j-1)}\mathbf{T}_{Dij}, i = 1, 2, j = 1, 2, \cdots, 6 \quad (2) $$

The detailed Denavit-Hartenberg parameters of one Omni device are shown in the TABLE I. It is worth noting that the θ_{i4} and θ_{i5} joints have limited ranges while the θ_{i6} joint has the biggest rotation range.

TABLE I
DENAVIT-HARTTENBERG PARAMETERS OF THE OMNI DEVICE

Index j	Parameters and Value Ranges			
	α_{j-1}	a_{j-1}	d_j	θ_{ij}
1	0°	0	135mm	$\theta_{i1} \in$ [-55°, 55°]
2	-90°	0	0	$\theta_{i2} \in$ [-101°, 0°]
3	0°	137mm	0	$\theta_{i3} \in$ [108°, 223°]
4	90°	0	137mm	$\theta_{i4} \in$ [-133°, 133°]
5	-90°	0	0	$\theta_{i5} \in$ [-154°, -17°]
6	90°	0	0	$\theta_{i6} \in$ [-146°, 146°]

C. Design and Optimization of the New Stylus

Two Omni devices are connected to construct the CombOmni. An intuitive connection is to simply connect the original styluses coaxially, as shown in Fig. 3. One could soon find out that this connection is far from the optimum.

Orientation of the axis of the original stylus is determined mainly by the θ_{i4} and θ_{i5} joints (affected by the θ_{i1}, θ_{i2} and θ_{i3} joints). The joint motion ranges are listed in Table I. Then the reachable orientations of the axis of the original stylus in the view of $\{Di3\}$ could be visualized in Fig. 3(a). The red area is reachable.

If the original styluses are connected coaxially, this limited reachable orientation range would severely limit the workspace of the CombOmni.

It is highly preferred that the axis of the new stylus could be oriented arbitrarily, when the new stylus is used to connect two Omni devices.

For this reason, the stylus elbow is introduced in the new stylus design, as shown in Fig. 2(a). As shown in Fig. 2(c), the axis of the original stylus ($\hat{\mathbf{z}}_{Di6}$) is rotated to the axis of the new stylus ($\hat{\mathbf{z}}_{Si2}$) by two rotations of δ_1 and δ_2.

Referring to Fig. 2(c), the δ_1 angle is the rotation angle from $\{Di6\}$ to $\{Si1\}$ about their shared X axes ($\hat{\mathbf{x}}_{Di6} = \hat{\mathbf{x}}_{Si1}$). The δ_2 angle is the rotation angle from $\{Si1\}$ to $\{Si2\}$ about the shared Y axes ($\hat{\mathbf{y}}_{Si1} = \hat{\mathbf{y}}_{Si2}$). The $\hat{\mathbf{z}}_{Si2}$ axis coincides with the new stylus handle axes ($\hat{\mathbf{z}}_{H1} = \hat{\mathbf{z}}_{H2}$).

The introduction of the stylus elbow is the key design idea. With the stylus elbow, the stylus axis now depends on not only θ_{i4} and θ_{i5}, but also θ_{i6}. Essentially, the θ_{i6} joint range is now utilized so that the axis of the new stylus can be arbitrarily oriented. Then the axis of the new stylus is addressed to have so-called *omnidirectional reachability*.

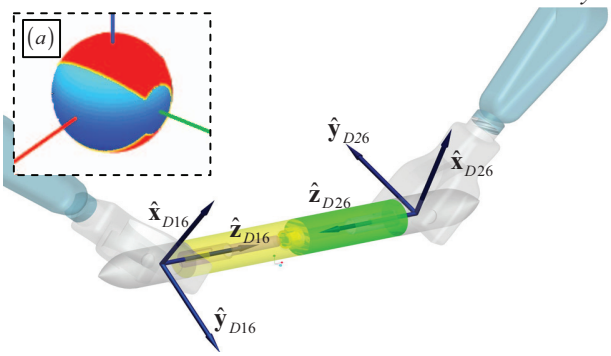

Fig. 3. An intuitive yet less optimal connection between two Omni devices: (a) the reachable orientations (in red) of the axis of the original stylus

Infinite pairs of the δ_1 and δ_2 angles would enable the omnidirectional reachability of the axis of the new stylus. An optimization is hence carried out as follows to determine the δ_1 and δ_2 values.

With the stylus elbow, the coordinate transformation matrix $ {}^{Di3}\mathbf{R}_{Si2}$ is written as in Eq. (3). $ {}^{Di3}\mathbf{R}_{Si2}$ could also be parameterized by the ZYZ Euler angles (φ_1, φ_2, and φ_3) as in Eq. (4).

$$ {}^{Di3}\mathbf{R}_{Si2} = {}^{Di3}\mathbf{R}_{Di6}(\theta_{i4}, \theta_{i5}, \theta_{i6})\mathbf{R}_{\hat{\mathbf{x}}}(\delta_1)\mathbf{R}_{\hat{\mathbf{y}}}(\delta_2) \quad (3) $$

$$ {}^{Di3}\mathbf{R}_{Si2} = \mathbf{R}_{\hat{z}}(\varphi_1)\mathbf{R}_{\hat{y}}(\varphi_2)\mathbf{R}_{\hat{z}}(\varphi_3) \quad (4) $$

Where $ {}^{Di3}\mathbf{R}_{Di6}$ can be extracted from Eq. (2); $\mathbf{R}_{\hat{\mathbf{x}}}$, $\mathbf{R}_{\hat{\mathbf{y}}}$ and $\mathbf{R}_{\hat{z}}$ are simple rotations about the $\hat{\mathbf{x}}$, $\hat{\mathbf{y}}$ and $\hat{\mathbf{z}}$ axes respectively.

Omnidirectional reachability of the axis of the new stylus depends on the δ_1 and δ_2 angles. For a pair of given δ_1 and δ_2 values, it means that there always exist a set of the θ_{i4}, θ_{i5} and θ_{i6} values within their joint limits for arbitrary φ_1 and φ_2 values. Then the optimization for determining the δ_1 and δ_2 values maximizes the averaged φ_3 range over the entire φ_1 and φ_2 ranges. The implementation is as follows in an enumerative manner.

The δ_1 and δ_2 values are varied within [-90°, 90°] in increments of 1°. Then for a pair of the δ_1 and δ_2 values, the

φ_1 and φ_2 values are varied in increments of 5° to generate all possible directions of the axis of the new stylus. The δ_1 and δ_2 value pair is admitted only if for each axis direction generated by the φ_1 and φ_2 angles, there exists at least one φ_3 value under which the θ_{i4}, θ_{i5} and θ_{i6} values obtained from Eq. (5) are within their joint limits.

$$^{Di3}\mathbf{R}_{Di6}(\theta_{i4},\theta_{i5},\theta_{i6}) = \mathbf{R}_{\hat{z}}(\varphi_1)\mathbf{R}_{\hat{y}}(\varphi_2)\mathbf{R}_{\hat{z}}(\varphi_3)\mathbf{R}_{\hat{y}}(-\delta_2)\mathbf{R}_{\hat{x}}(-\delta_1) \quad (5)$$

Then the averaged range of the φ_3 angle in all the axis directions generated by the φ_1 and φ_2 angles are plotted in Fig. 4 with respect to the δ_1 and δ_2 values.

It can be seen from Fig. 4 that there are four optimal scenarios. They are equivalent since they are symmetric in the plotting coordinate. Then the scenario of $\delta 1$ = 37° and $\delta 2$ = -37° is adopted. In this optimal scenario, the averaged φ_3 value is 202.1°.

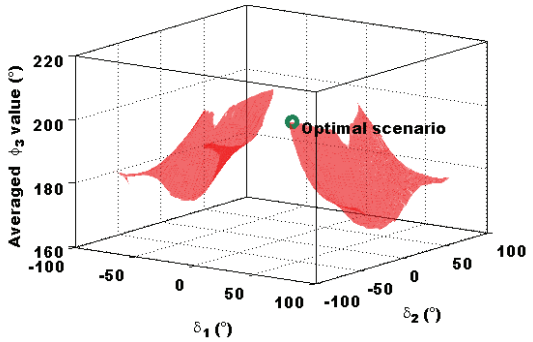

Fig. 4. Design optimization of the stylus elbow

D. Optimized Arrangement of the Two Omni Devices

With the help of the stylus elbow, the new stylus axis can now be arbitrarily oriented. Due to the fact that the θ_{i6} angle is partially used to orient the stylus axis, the new stylus has a reduced rotation range about its own axis. Hence an additional joint is added between the stylus handle and the stylus elbow. The mechanism is explained in Section III.

The handle coordinate $\{Hi\}$ is attached to the stylus handle which is installed on the stylus elbow of the i^{th} Omni device, referring to Fig. 2(c). $\{Hi\}$ is rotated from $\{Si2\}$ for an angle of θ_{Hi}. $\{H1\}$ and $\{H2\}$ share their Z axes and the origins. The origins of $\{Hi\}$ is now the input point of the CombOmni, while the orientations of $\{H1\}$ and $\{H2\}$ could simulate the jaws of a medical instrument in a robotic surgery.

It is obviously desirable that the length of the new stylus (distance between the gimbal centers of the two Omni devices) is shorter in order to generate bigger workspace of the CombOmni. As explained in Section III, the distance is set 80mm, considering the necessary components and avoidance of interference.

The next optimization determines the relative positioning of the two Omni devices, in order to better utilize their given workspace. For the sake of convenience in assembly and use, the two Omni devices are assumed to be placed face-to-face in the $\hat{\mathbf{x}}_W$ direction on the same plane. Then three arrangement parameters should be determined: the relative positioning (p_x and p_y) and orientation (γ) of the 2^{nd} Omni device with respect to the 1^{st} one.

With the stylus elbows and the stylus handles installed, the workspace (W-1) of the 1^{st} Omni device concerning the gimbal center of the 2^{nd} Omni device, in $\{D10\}$, is firstly generated, scanning the joint space of the 1^{st} Omni device.

Then the workspace (W-2) of the 2^{nd} Omni device concerning its own gimbal center, in $\{D20\}$, is generated. Moving the 2^{nd} Omni device also translates and rotates its workspace at the same time. When the 2^{nd} Omni device is placed with respect to the 1^{st} one, the size of the overlapped volume of the workspace W-1 and the mobilized workspace W-2 could be obtained. The arrangement of the 2^{nd} Omni device with respect to the 1^{st} one is determined when the overlapped workspace volume reaches its maximum.

The p_x, p_y and γ values are enumerated within [200mm, 500mm] and [0°, 180°] in increments of 20mm and 10°. The overlapped workspace is maximized when $[p_x\, p_y\, \gamma]$ = [360mm 0mm 180°]. The workspace of the CombOmni is then plotted in Fig. 5.

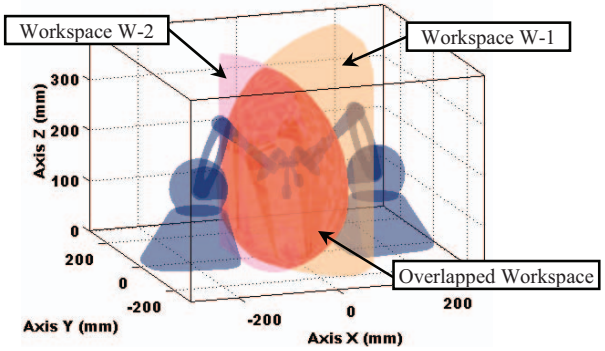

Fig. 5. Workspace of the CombOmni

With the arrangement of the 2^{nd} Omni device with respect to the 1^{st} one determined, the complete kinematics of the CombOmni can be detailed as follows.

The base of the 1^{st} Omni device $\{D10\}$ is located at $^{W}\mathbf{p}_{D10}$ =[-180mm 0 0]^T in $\{W\}$, while the 2^{nd} one $\{D20\}$ is placed at $^{W}\mathbf{p}_{D20}$ =[180mm 0 0]^T in $\{W\}$. $\hat{\mathbf{x}}_{D10}$ and $\hat{\mathbf{x}}_{D20}$ are in the opposite directions.

Then the homogeneous transformation matrix of $\{H1\}$ in $\{W\}$ could be obtained as in Eq. (6).

$$^{W}\mathbf{T}_{H1} = \begin{bmatrix} \mathbf{I}_{3\times3} & ^{W}\mathbf{p}_{D10} \\ \mathbf{0}_{1\times3} & 1 \end{bmatrix} \cdot {}^{D10}\mathbf{T}_{S12} \cdot \begin{bmatrix} \mathbf{R}_{\hat{z}}(\theta_{H1}) & ^{S12}\mathbf{p}_{H1} \\ \mathbf{0}_{1\times3} & 1 \end{bmatrix} \quad (6)$$

Where $^{D10}\mathbf{T}_{S12} = {}^{D10}\mathbf{T}_{D16} \cdot \begin{bmatrix} \mathbf{R}_{\hat{x}}(\delta_1)\mathbf{R}_{\hat{y}}(\delta_2) & \mathbf{0}_{3\times1} \\ \mathbf{0}_{1\times3} & 1 \end{bmatrix}$, θ_{H1} is the rotation angle between $\{S12\}$ and $\{H1\}$. θ_{H1} is measured by the rotary potentiometer as explained in Section III.

Similarly, the handle frame $\{H2\}$ is attached to the inner handle. The transformation matrix could be derived as in (7).

$$ {}^{W}\mathbf{T}_{H2} = \begin{bmatrix} \mathbf{R}_{\hat{z}}(\pi) & {}^{W}\mathbf{p}_{D20} \\ \mathbf{0}_{1\times3} & 1 \end{bmatrix} \cdot {}^{D20}\mathbf{T}_{S22} \cdot \begin{bmatrix} \mathbf{R}_{\hat{x}}(\pi)\mathbf{R}_{\hat{z}}(\theta_{H2}) & {}^{S22}\mathbf{p}_{H2} \\ \mathbf{0}_{1\times3} & 1 \end{bmatrix} \quad (7) $$

Where θ_{H2} is the rotation angle between $\{S22\}$ and $\{H2\}$, and ${}^{D20}\mathbf{T}_{S22} = {}^{D20}\mathbf{T}_{D26} \cdot \begin{bmatrix} \mathbf{R}_{\hat{x}}(\delta_1)\mathbf{R}_{\hat{y}}(\delta_2) & \mathbf{0}_{3\times1} \\ \mathbf{0}_{1\times3} & 1 \end{bmatrix}$.

III. System Description of the CombOmni

The CombOmni consists of two Omni devices whose relative positioning is determined as in Section II.D. Referring to the relative positioning, an acrylic board was firstly cut to mount the two Omni devices.

The original stylus of the Omni device can be easily unplugged as shown in Fig. 6(a). Apparently a 6.35mm stereo audio jack plug was used to connect the original stylus. Since the distance between the two gimbal centers should be as short as possible to increase the workspace, this connector was hence shortened as shown in Fig. 6(b), in order to reduce possible motion interference.

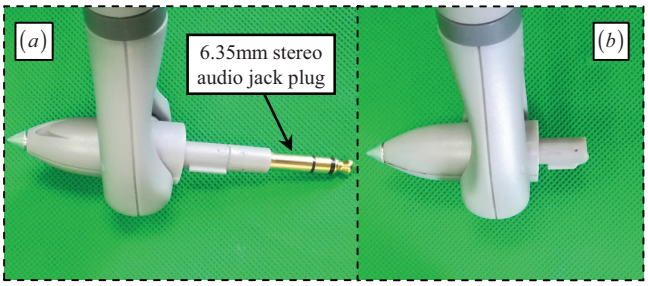

Fig. 6. Modification of the Omni device for connection: (a) original stylus connector, and (b) shortened stylus connector

The new stylus was used to connect the two Omni devices. It consists of two stylus elbows, two stylus handles, two potentiometers and a couple of miscellaneous components.

The stylus elbow is installed on the shortened stylus connector that is shown in Fig. 6(b). A screw is tightened to lock the stylus elbow on the connector, as shown in Fig. 7.

Then the following components are assembled axially on a Ø2mm central shaft, referring to Fig. 7(a): a pair of miniature bearings, a cover plate, a potentiometer (muRata SV01A1), the stylus elbow, the stylus handle, a torsional spring, the other stylus handle, the other stylus elbow, a second potentiometer, a second cover plate, and a second pair of miniature bearings. Two nuts are tightened on the two ends of the shaft to axially fix all the components.

The stylus elbow provides housing for the potentiometer that is retained by the cover plate. A channel is reserved in the stylus elbow to pass the wires of the potentiometer. A D-shaped shoulder is extruded into the potentiometer so that rotation of the stylus handle will be measured by the potentiometers. The two measured angles (θ_{H1} and θ_{H2}) between the stylus elbow and the stylus handles are necessary for calculating the kinematics of the stylus handles.

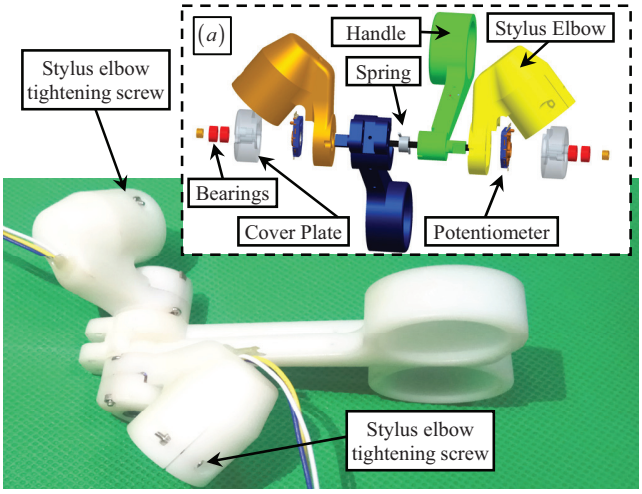

Fig. 7. The new stylus of the CombOmni: (a) an exploded view of the components

A computer (e.g., a desktop PC) would be needed to connect the CombOmni's two Omni devices. The connection is via IEEE 1394 bus. APIs (Applications Programming Interface) are available from the OpenHaptic™ libraries for reading the joint values and poses of the Omni devices, as well as generating programmed forces at the gimbal centers.

In the presented setting, a multi-function card (Advantech PCI-1710) was plugged into the desktop PC for reading the voltages of the potentiometers in the new stylus. The ADC conversion has a resolution of 12 bits. A resolution of 0.08° could be achieve by reading from the potentiometer.

IV. Preliminary Experimentation

To verify the effectiveness of the proposed CombOmni design, preliminary experimentation was carried out.

As shown in Fig. 8, a Denso manipulator was used to hold and mobilize the new stylus of the CombOmni inside the CombOmni's workspace. The advantage of using a Denso manipulator over manual movements is mainly that the Denso manipulator provides smooth, steady and repeatable movements.

Two markers were attached to the stylus handle and the base of the CombOmni, respectively. Then positions and orientations of the stylus handle in $\{W\}$ were read by an optical tracker (Micron Tracker SX60 from Claron Technology Inc.). The recorded movements of the CombOmni's new stylus are plotted in Fig. 9(a).

Via the APIs of the Omni devices and the potentiometer readings, positions and orientations of the stylus handle can be calculated using Eq. (6). These calculated positions are also plotted in Fig. 9(a). The errors between the tracked positions and the calculated positions, characterized as the *reading errors* of the CombOmni, are plotted in Fig. 9(b). It can be seen that these reading errors are mostly under 0.15mm. The position resolution of the Omni device is 0.06mm from the datasheet. The tracking accuracy of the

optical tracker might have contributed to the measurement discrepancy.

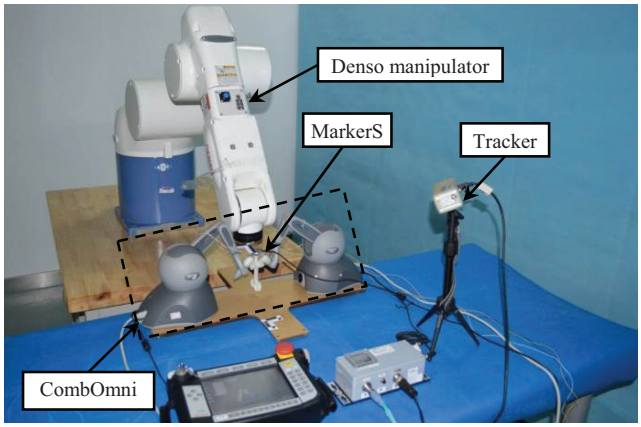

Fig. 8. Pose read-outs of the CombOmni held by a Denso manipulator

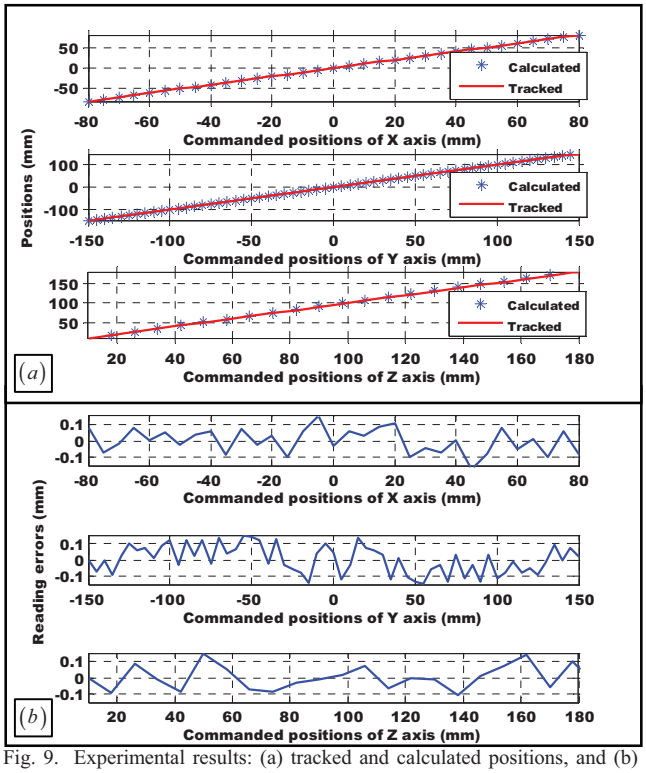

Fig. 9. Experimental results: (a) tracked and calculated positions, and (b) reading errors

V. Conclusions and Future Work

This paper presents the design, optimization, system construction and preliminary experimentation of the CombOmni, a haptic device for teleoperation applications.

The main motivation is to provide an affordable and simple solution for vast researcher population who do not have sufficient access to haptic devices with both force and torque outputs: the products are too expensive and the research prototypes are difficult to reproduce.

The key design element is the introduction of a stylus elbow which optimally uses the available joint ranges to facilitate the connection between two Omni devices. With the arrangement of the two Omni devices optimized, the CombOmni fully utilizes the capabilities of the Omni devices.

Extensive experimentation would be carried out to characterize the specifications of the CombOmni, including translational and dexterous workspace, force and wrench output, etc. With the capabilities fully demonstrated, the CombOmni could become a viable option for a haptic device with both force and torque outputs in a cost-effective way.

References

[1] B. Hannaford and A. M. Okamura, "Haptics," in *Springer Handbook of Robotics*. vol. Part D, B. Siciliano and O. Khatib, Eds.: Springer, 2008, pp. 719-739.

[2] J. Arata, H. Kondo, N. Ikedo, and H. Fujimoto, "Haptic Device Using a Newly Developed Redundant Parallel Mechanism," *IEEE Transactions on Robotics,* vol. 27, No.2, pp. 201-214, 2011.

[3] R. Steger, K. Lin, B. D. Adelstein, and H. Kazerooni, "Design of a Passively Balanced Spatial Linkage Haptic Interface," *Journal of Mechanical Design,* vol. 126, No.6, pp. 984-991, 2004.

[4] L. Birglen, C. Gosselin, N. Pouliot, B. Monsarrat, and T. Laliberté, "SHaDe, a New 3-DOF Haptic Device," *IEEE Transactions on Robotics and Automation,* vol. 18, No.2, pp. 166-175, April 2002.

[5] G. Tholey and J. P. Desai, "A General-Purpose 7 DOF Haptic Device: Applications Toward Robot-Assisted Surgery," *IEEE/ASME Transactions on Mechatronics,* vol. 12, No.6, pp. 662-669, Dec 2007.

[6] G. L. Long and C. L. Collins, "A Pantograph Linkage Parallel Platform Master Hand Controller for Force-Reflection," in *IEEE International Conference on Robotics and Automation (ICRA)*, Nice, France, 1992, pp. 390-395.

[7] Y. Tsumaki, H. Naruse, D. N. Nenchev, and M. Uchiyama, "Design of a Compact 6-DOF Haptic Interface," in *IEEE International Conference on Robotics and Automation (ICRA)*, Leuven, Belglum, 1998, pp. 2580-2585.

[8] L. J. Stocco, S. E. Salcudean, and F. Sassani, "Optimal Kinematic Design of a Haptic Pen," *IEEE/ASME Transactions on Mechatronics,* vol. 6, No.3, pp. 210-220, Sept 2001.

[9] M. Ueberle and M. Buss, "Design,Control,and Evaluation of a New 6 DOF Haptic Device," in *IEEE/RSJ International Conference on Intelligent Robots and Systems (IROS)*, Lausanne, Switzerland, 2002, pp. 2949-2954.

[10] K. Kim and W. Kyun, "Design and Analysis of a New 7-DoF Parallel Type Haptic Device: PATHOS-II," in *IEEE/RSJ International Conference on Intelligent Robots and Systems (IROS)*, 2003, pp. 2241-2246.

[11] E. L. Faulring, J. E. Colgate, and M. A. Peshkin, "The Cobotic Hand Controller: Design, Control and Performance of a Novel Haptic Display," *International Journal of Robotics Research,* vol. 25, No.11, pp. 1099-1119, 2006.

[12] N. Bernstein, D. Lawrence, and L. Pao, "Dynamics Modeling for Parallel Haptic Interfaces with Force Sensing and Control," *IEEE Transactions on Haptics,* vol. 6, No.4, pp. 429-439, 2013.

[13] Z. Najdovski, S. Nahavandi, and T. Fukuda, "Design, Development, and Evaluation of a Pinch–Grasp Haptic Interface," *IEEE/ASME Transactions on Mechatronics,* vol. 19, No.1, pp. 45-54, 2014.

[14] G. Lee, S.-M. Hur, and Y. Oh, "A Novel Haptic Device with High-Force Display Capability and Wide Workspace," in *IEEE International Conference on Robotics and Automation (ICRA)*, Stockholm, Sweden, 2016, pp. 2704-2709.

[15] Y. Lin and Y. Sun, "5-D Force Control System for Fingernail Imaging Calibration," in *IEEE International Conference on Robotics and Automation (ICRA)*, Shanghai, China, 2011, pp. 1374-1379.

[16] Y. Kobayashi, Y. Sekiguchi, T. Noguchi, Y. Takahashi, Q. Liu, S. Oguri, K. Toyoda, M. Uemura, S. Ieiri, M. Tomikawa, T. Ohdaira, M. Hashizume, and M. G. Fujie, "Development of a Robotic System with Six-Degrees-of-Freedom Robotic Tool Manipulators for Single-Port Surgery," *International Journal of Medical Robotics and Computer Assisted Surgery,* vol. 11, No.2, pp. 235-246, June 2015.